Glasslike behavior at the $PrBa_2Cu_3O_7/La_{0.75}Sr_{0.25}MnO_3$ interface

N. Haberkorn, F. Lovey, A. M. Condó, G. Nieva, and J. Guimpel
Comisión Nacional de Energía Atómica, Centro Atómico Bariloche, Instituto Balseiro, Universidad Nacional de Cuyo and Comisión Nacional de Energía Atómica, S. C. de Bariloche, 8400 R. N., Argentina
(Received 21 June 2006; revised manuscript received 28 September 2006; published 24 January 2007)

We study the crystalline structure and the magnetic properties of two different $PrBa_2Cu_3O_{7-\delta}/La_{0.75}Sr_{0.25}MnO_3$ ($PBCO/LSr_{0.25}MO$) superlattices grown by dc magnetron sputtering on (100) $SrTiO_3$. The microstructure was studied by high-resolution transmission electron microscopy (HRTEM). Magnetic, magnetotransport, and time dependence measurements indicate a behavior compatible with phase separation at the interface, strain induced by the lattice parameter difference, and the presence of a structural transition in the manganite material. Spin glasslike blocking behavior was found at low temperatures, below 70 K.

DOI: 10.1103/PhysRevB.75.024427 PACS number(s): 75.70.Cn, 75.30.Kz, 68.65.Cd, 75.50.Lk

INTRODUCTION

The role of the different interfacial disorder mechanisms on the physical properties of perovskite superlattices, such as interdiffusion, stress, oxygen deficiency, or charge transfer, is an important point to be studied.[1–4] As an example, in $La_{2/3}Ca_{1/3}MnO_3/La_{2/3}Sr_{1/3}MnO_3$ ($LCa_{1/3}MO/LSr_{1/3}MO$) superlattices, interfacial strain induces a phase separation with suppressed ferromagnetism.[5] In a previous work, we showed that the interface between $La_{1-x}A_xMnO_3$ manganites (LA_xMO with A: Sr, Ca; Ba; $0.2<x<0.5$) and $RBa_2Cu_3O_{7-\delta}$ (RBCO with R: Y, Gd) superconductors affects the magnetic properties of both materials. In the LA_xMO layers saturation magnetization (M_S) and Curie temperature (T_C) are reduced from bulk values, whereas in the RBCO layers the superconducting temperature (T_S) is also reduced from that of the bulk.[1–3] In particular, for LA_xMO/RBCO superlattices an unexpected antiferromagnetic (AF) phase appears at the interface.[6,7] These could be a consequence of a shift in the Mn^{3+}/Mn^{4+} relation towards Mn^{4+}, and consequently towards the AF manganite phase, probably due to a hole transfer from the RBCO to the manganite.[8,9] The physical properties of the interface material could then be modified by the charge density of the layers. The $PrBa_2Cu_3O_{7-\delta}$ (PBCO) is structurally isomorphic to the superconducting RBCO but with an insulatorlike behavior. Therefore PBCO offers the possibility of growing $LA_xMO/PBCO$ superlattices with a similar crystalline structure but with different charge balance between layers as from LA_xMO/RBCO superlattices.

We have previously shown for $LSr_{0.25}MO/PBCO$ superlattices that M_S is smaller than the nominal value,[10] similar to what was found in ferromagnetic LA_xMO/RBCO. However, the presence of AF behavior was not detected. Instead, we found evidence of frustrated magnetism at the interfaces. In this work, we extend the study of the $LSr_{0.25}MO/PBCO$ system in order to characterize the magnetic behavior at the interface and its correlation to the overall physical properties. We investigate the microstructure, magnetic properties, and magnetotransport for two particular $LSr_{0.25}MO/PBCO$ superlattices where the $LSr_{0.25}MO$ layer thickness is such that the frustrated behavior is clearly observed.

Our results show a spin glasslike (SGL) behavior at low temperature similar to that found in $La_{1-x-y}Pr_yCa_xMnO_3$.[11] In our case the SGL behavior is strain induced, due to the presence of an orthorhombic-rhombohedric structural phase transition in the manganite.[12]

EXPERIMENTAL DETAILS

The $LSr_{0.25}MO/PBCO$ superlattices were grown on (100) $SrTiO_3$ (STO) by dc magnetron sputtering, as previously reported.[13] For all superlattices the starting layer is a 6 unit cell (u.c.) thick PBCO buffer layer, which was included in order to have all the $LSr_{0.25}MO$ layers in contact with PBCO at both interfaces. In the following, the superlattices are labeled as $[L_MP_N]_L$, where M and N indicates the $LSr_{0.25}MO$ and PBCO layer thickness in u.c., respectively, and L indicate the number of bilayers. In this work we analyzed two different superlattices $(M,N,L)=(18,6,5)$ and (31, 6, 4). To distinguish the different types of interfaces we use layer 1/layer 2 convention that means that layer 2 was grown on top of layer 1.

The crystalline structure of the superlattices was studied using high-resolution transmission electron microscopy (HRTEM). Specimens were prepared as reported elsewhere.[14] We show the results for the superlattice $(M,N,L)=(18,6,5)$, that we consider representative. The structure of fully oxidized PBCO corresponds to an orthorhombic $Pmmm$ system, with lattice parameters: $a\approx0.3928$ nm, $b\approx0.3878$ nm, and $c\approx1.1718$ nm. The structure of the $LSr_{0.25}MO$ corresponds to the hexagonal—rhombohedral $R\bar{3}C$ system, with lattice parameter, $a_h\approx0.547$ nm and $c_h\approx1.33$ nm, usually described with a pseudocubic lattice with $a_c\approx0.386$ nm. In order to interpret the experimental HRTEM results, image simulations were performed constructing supercells containing various possible interface stacking sequences. The images were simulated using the multislice method in the electron microscopy simulation (EMS) package given by Stadelmann.[15]

Magnetization (M) vs temperature (T) measurements and hysteresis loops were measured in a commercial superconducting quantum interference device (SQUID). M vs T data were obtained for both superlattices and a reference $LSr_{0.25}MO$ film, at a magnetic field (H) of 50 Oe under field

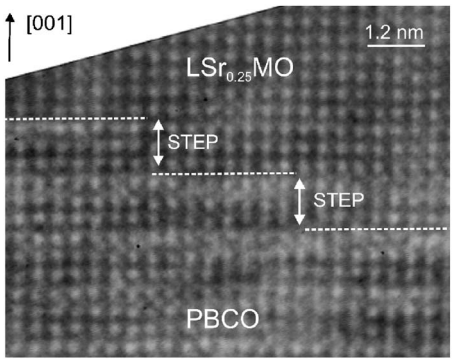

FIG. 1. Two consecutive steps at the PBCO/$LSr_{0.25}MO$ interface. White dashed lines in the picture indicate the interface between both materials. The image was taken along the $[0\bar{1}0]$ zone axis.

cooling conditions (FC). The hysteresis loops were taken at several temperatures in the -10 kOe$<H<10$ kOe range.

Magnetotransport was measured with the conventional four-probe geometry with the magnetic field (H) parallel to the surface. The data was acquired on warming up after different magnetic history preparations: (1) $H=0$; after zero field cooling; (2) $H=5$ kOe, after zero field cooling (ZFC); (3) $H=5$ kOe, after cooling with $H=5$ kOe (FC); and (4) $H=0$ after cooling with $H=5$ kOe (REM).

The resistivity of the superlattices was calculated in base to total thickness. The resistivity time relaxation (RR) measurements were performed at $H=5$ KOe and $H=0$. For the RR measurement the samples were ZFC from room temperature, and, when the temperature was stabilized, a magnetic field of $H=5$ kOe was applied for different waiting times (t_w) between 60 s and 18 000 s. The magnetic field was then reduced to zero and the relaxation data were recorded for time intervals longer than 10^4 s. To avoid errors due to the relaxation of the residual field in the magnet, the cryostat was removed from it prior to perform the resistivity time-dependent measurements.

RESULTS

Crystalline structure

We have identified only one epitaxy between PBCO and the substrate, which corresponds to [100] PBCO‖[100] STO. The interface discrete disorder is around 1 u.c. of PBCO at the PBCO/$LSr_{0.25}MO$ interface and 1 u.c. of $LSr_{0.25}MO$ in the $LSr_{0.25}MO$/PBCO interface. Figure 1 shows two neighboring steps of 1 u.c. of PBCO in the PBCO/$LSr_{0.25}MO$ interface. These neighboring steps could be originated as a consequence of the PBCO island nucleation during growth.[16]

The average thickness of the $LSr_{0.25}MO$ and PBCO layers in the $[L_{18}P_6]_5$ superlattice, measured from the HRTEM images, is in the range 15–18 u.c. for $LSr_{0.25}MO$, and in the range 6–8 u.c. for the PBCO layers. One PBCO layer showed an unexpected larger thickness of 9–11 u.c. In this particular layer we observed PBCO grains with [100] or [010] epitaxy. These grains have a lateral size smaller than 10 nm, and always nucleate on (001) PBCO. Given the small amount, and considering that they were only found in one of the layers, we do not think they have a significant influence on the physical properties of the superlattice.

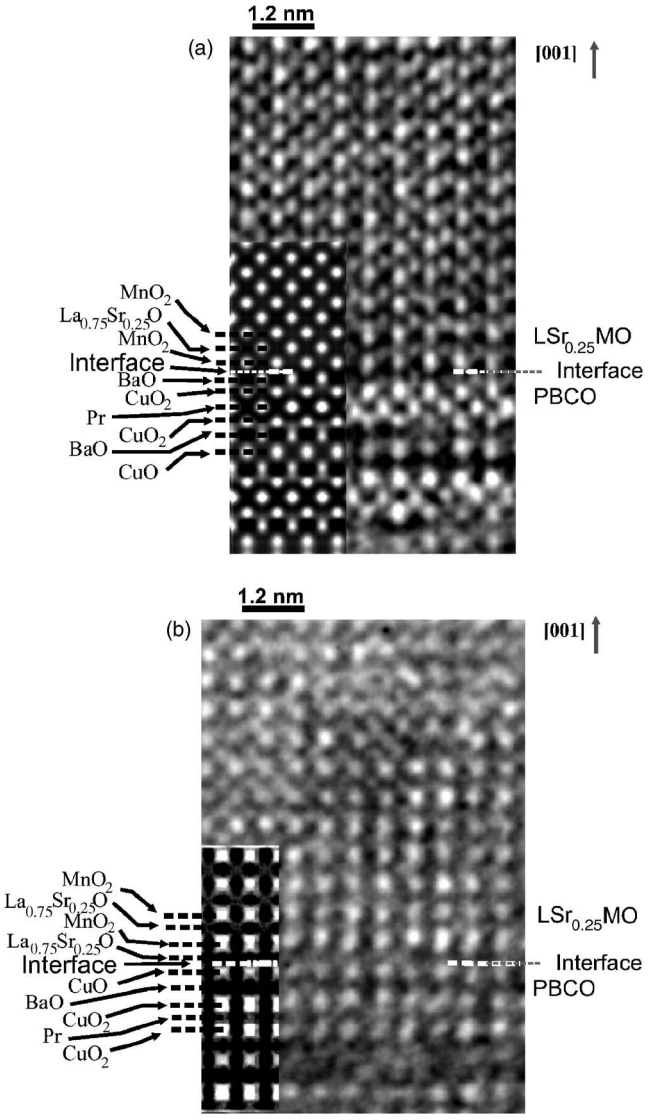

FIG. 2. PBCO/$LSr_{0.25}MO$ interface from the $[0\bar{1}0]$ direction. The insets correspond to the simulated image. (a) Interface with stacking sequence CuO_2-BaO-MnO_2. The simulated image corresponds to defocus and thickness values of -36 nm and 2.2 nm, respectively. (b) Interface with stacking BaO-Cu-$LSr_{0.25}O$. The simulated image corresponds to defocus and thickness values of -46 nm and 5 nm, respectively.

In order to analyze the stacking plane sequence in the PBCO/$LSr_{0.25}MO$ and $LSr_{0.25}MO$/PBCO interfaces, the experimental pictures were compared with simulated images for different models, as explained in Ref. 14. The HRTEM images of the PBCO/$LSr_{0.25}MO$ interface show two different stacking sequences, shown in Fig. 2. One is formed when a PBCO layer finishes in a sequence Pr-CuO_2-BaO plane, and $LSr_{0.25}MO$ starts with a MnO_2 plane, see Fig. 2(a). The second type of interface observed corresponds to a sequence where the CuO-chains plane faces a $LSr_{0.25}O$ plane, see Fig. 2(b). The $LSr_{0.25}MO$/PBCO interface also shows two

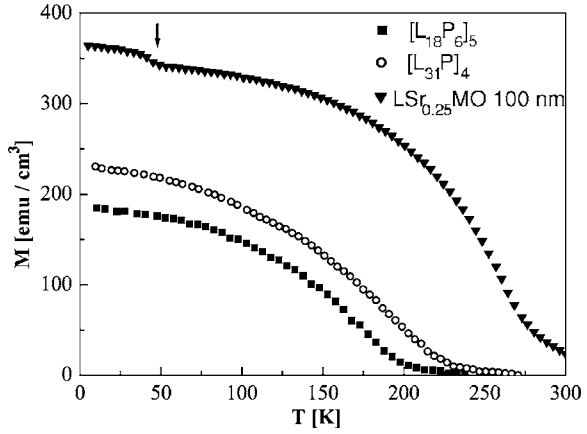

FIG. 3. Magnetization (M) vs temperature (T) with a magnetic field $H=50$ kOe for $[L_{18}P_6]_5$ and $[L_{31}P_6]_4$ superlattices and a reference $LSr_{0.25}MO$ 100 nm thick film.

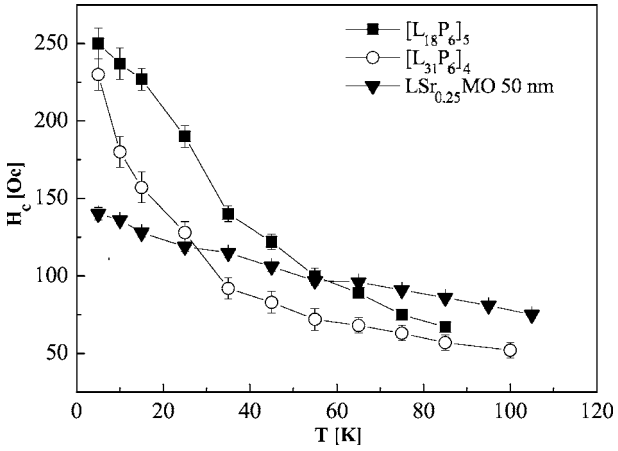

FIG. 4. Coercive field (H_c) vs temperature (T) for $[L_{18}P_6]_5$ and $[L_{31}P_6]_4$ superlattices, and a reference $LSr_{0.25}MO$ 50 nm thick film.

stacking plane sequences, mirror to those of the PBCO/$LSr_{0.25}MO$ one. One is formed when a $LSr_{0.25}MO$ finishes with a MnO_2 plane and the PBCO layer starts in a sequence BaO-CuO_2-Pr planes (not showed). The second kind of interface corresponds to a sequence where a $LSr_{0.25}O$ plane faces a CuO chains plane (not shown). We also observed another type of interface provided by the presence of the PBCO [100] or [010] grains mentioned earlier. In this interface the PrO or BaO layers face MnO_2 or CuO_2 and CuO chains face $LSr_{0.25}O$ layers.

Magnetic measurements

Magnetization vs temperature (M vs T) measurements at 50 Oe for $[L_{18}P_6]_5$ and $[L_{31}P_6]_4$ superlattices and for a reference $LSr_{0.25}MO$ 100 nm thick film are shown in Fig. 3. The measured reference films of thickness 100 nm and 50 nm, the last not included in the figure, present a shoulder in the M vs T curve at 50 K, pointed by the arrow in Fig. 3. We associate this shoulder to a structural transition since the $La_{0.75}Sr_{0.25}MnO_3$ composition is near to the orthorhombic-rhombohedral boundary for bulk samples.[12] Both phases are reported to be ferromagnetic but with different magnetic anisotropy,[17] which originates a shoulder in the M vs T curves, such as the one observed in Fig. 3. The shoulder is not observed for the superlattices.

The M_S (from hysteresis loops) and T_C for the $[L_{18}P_6]_5$ and $[L_{31}P_6]_4$ superlattices are 210(20) emu/cm3, 200(10) K and 320(20) emu/cm3, 225(10) K, respectively.[10] The coercive field (H_c) temperature dependence for the superlattices and for the 50 nm reference film are shown in Fig. 4.

Magnetotransport

Figure 5 shows the temperature dependence of the resistivity for the reference $LSr_{0.25}MO$ 50 nm thick film. Although barely visible, the anomaly at 50 K related to the structural transition mentioned previously, is present in the data. The magnetoresistance at 5 KOe, $\Delta\rho=[\rho_{5\ KOe}-\rho_{H=0}]/\rho_{H=0}$, is also shown in Fig. 5. A measurable difference between FC and ZFC magnetoresistance is not found in the examined temperature range.

As previously reported, the electrical resistivity of $LSr_{0.25}MO$/PBCO superlattices can be described with a simple parallel resistor model.[10] Figure 6(a) shows resistivity (ρ) vs T, and Figs. 6(b) and 6(c) show $\Delta\rho$ vs T, with $\Delta\rho=[\rho-\rho_{H=0}]/\rho_{H=0}$, for different magnetic field cooling conditions: $H=5$ kOe after ZFC ($\Delta\rho_{ZFC}$), $H=5$ kOe after FC ($\Delta\rho_{ZFC}$) or REM after FC at 5 kOe ($\Delta\rho_{REM}$). As we can see, at low temperatures the superlattices show unexpected differences between FC and ZFC curves. These differences appear at temperatures lower than approximately 70 K. A kink in the $\Delta\rho_{REM}$ and $\Delta\rho_{ZFC}$ curves is observed at approximately 40 K indicating an abrupt change in the conductivity of the superlattices. These anomalous differences between $\Delta\rho_{FC}$ and $\Delta\rho_{ZFC}$ curves in the superlattices occur in the same temperature range where the reference $LSr_{0.25}MO$ film shows the orthorhombic-rhombohedral phase transition. The electrical resistivity of the $LSr_{0.25}MO$/PBCO superlattices shows [down arrows in Fig. 6(a)] shoulders associated with the same structural phase transition.

These data are compatible with previous results on systems showing phase separation.[18–21] In those systems the

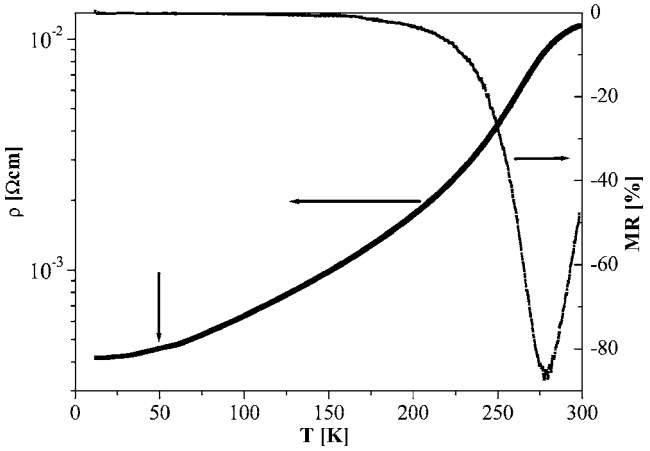

FIG. 5. Temperature dependence of the resistivity and $\Delta\rho$ [%] at 5 kOe for a reference $LSr_{0.25}MO$ 50 nm thick film.

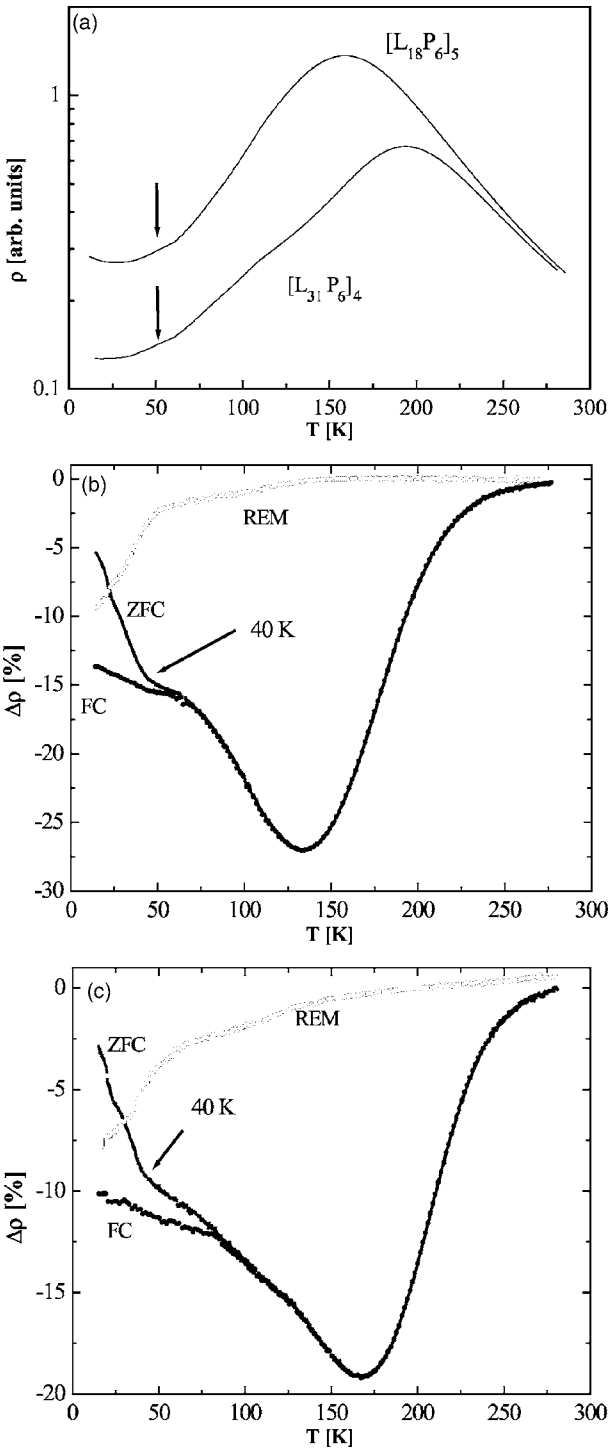

FIG. 6. (a) Resistivity (ρ) vs temperature (T) for $[L_{18}P_6]_5$ and $[L_{31}P_6]_4$ superlattices. (b) and (c) $\Delta\rho=[\rho-\rho_{H=0}]/\rho_{H=0}$, with $H=5$ kOe after ZFC ($\Delta\rho_{ZFC}$), $H=5$ KOe after FC ($\Delta\rho_{FC}$) or REM after FC at 5 KOe ($\Delta\rho_{REM}$) for $[L_{18}P_6]_5$ and $[L_{31}P_6]_4$ superlattices, respectively.

physical properties are determined by the dynamic coexistence of two or more magnetic or structural phases with blocking at low temperature.[18] Several works in manganites with phase separation reveal a spin glasslike (SGL) behavior at low temperatures.[19–21] A common way to detect SGL behavior is to perform magnetic relaxation measurements.[22]

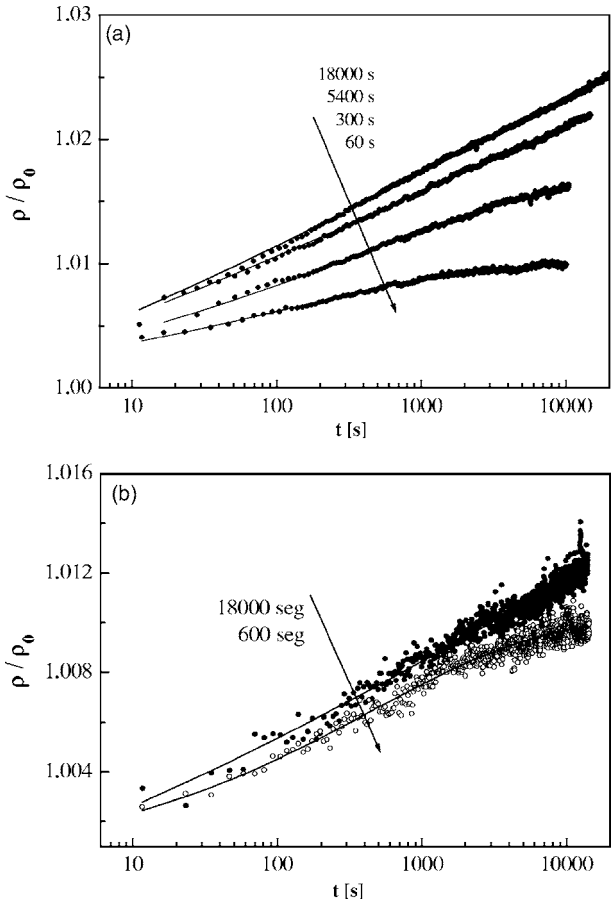

FIG. 7. Time dependence of the resistivity for different t_w at 25 K. (a) $[L_{18}P_6]_5$. (b) $[L_{31}P_6]_4$. Numbers indicate waiting times with field applied before removing it and measuring.

Due to the close relation between electrical transport and magnetization in manganites, resistivity vs time (t) measurements give an insight on the magnetic relaxation.[23]

Figures 7(a) and 7(b) show the magnetic relaxation for the studied superlattices at 25 K. The ratio $\rho(t)/\rho(t=0)$ is plotted for each sample. A clear influence of the waiting time (t_w) over the resistivity relaxation (RR) of the superlattices is evident. The figures also show fits for each curve using a stretched exponential $\Delta\rho=\Delta\rho_0\exp[-(t/\tau)^{\beta}]$, typical response of deeply disordered systems with a broad range of relaxation times. In the expression, t is the time after the magnetic field H was removed, τ is a relaxation time parameter, and the exponent β ranges between 0 and 1.

We have also observed that the t_w effects are less important for temperatures higher that 50 K. In this range of temperature the RR measurements show a higher noise as a consequence of the high $\partial\rho/\partial T$ which induces $\Delta\rho$ through the temperature fluctuations in our system (approximately 25 mK).

DISCUSSION

The structural results presented in this work for $LSr_{0.25}MO/PBCO$ show that the interfaces stacking are similar to those found in superconducting LA_xMO

$(A:Ca,Sr)/R$BCO $(R:Gd,Y)$ superlattices,[14,24] However $LSr_{0.25}$MO/PBCO superlattices do not show the presence of ferromagnetic/AF interfaces. Our results indicate, in turn, the presence of frustrated ferromagnetism at the $LSr_{0.25}$MO/PBCO interface, provided the large magnetoresistance at temperature much lower than the Curie temperature, in contrast with $LSr_{0.25}$MO reference films.

We have found the presence of SGL behavior, linked with stress changes induced by the orthorhombic-rhombohedral transition in the $LSr_{0.25}$MO layers. SGL behavior associated to strain was analyzed by Sharma *et al.* in $(La,Pr)_{5/8}Ca_{3/8}MnO_3$ manganites,[18] where a dynamic coexistence of FM and charge ordering (CO) phase is frozen as a consequence of long-range martensitic stress accommodation. The interfaces in thin films and superlattices are normally stressed due to lattice parameter mismatch. Thus, in magnetic manganite superlattices a SGL behavior could be expected provided that the local disorder favors a mixture of FM and non-FM regions (separation of dynamically intergrown phases).

The SGL behavior appears for temperature lower than approximately 70 K, where the superlattices show differences between FC and ZFC in resistivity vs T curves with an important kink at 40 K [Figs. 6(b) and 6(c)]. The onset of the blocking behavior at temperatures almost 20 K above the orthorhombic-rhombohedral transition in the reference films ($\approx$50 K) could be associated with two effects: a more stressed $LSr_{0.25}$MO atomic layers close to the interface; or charge transfer at the interfaces, since an increase in the Mn^{3+}/Mn^{4+} ratio could shift the transition to temperatures higher than 50 K.[12]

Another signature of the SGL behavior at the superlattice interfaces is the temperature dependence of the coercive fields (H_c). For the superlattices, H_c has a steeper upturn at low temperatures than the reference $LSr_{0.25}$MO film, as shown in Fig. 4. This indicates that the magnetic domain wall movement is hindered by the distorted interface material, and undergoes a transition to a blocked state. Models of weak or strong domain wall pinning,[25] do not describe the data in the measured temperature range for each sample, not even in the range where M_s remains approximately constant.

A point to be clarified is whether the observed SGL behavior is originating in a fraction of the manganite layers at the interfaces, or in the complete manganite layers. In addition to the two superlattices presented in detail in this paper, we have also measured other samples with different $LSr_{0.25}$MO layer thickness. We detect ferromagnetism for $LSr_{0.25}$MO layer thickness larger than 4 nm, which means that only above this thickness a ferromagnetic core is present. For very thick $LSr_{0.25}$MO layers (>12 nm) the magnetorresistance value at low temperatures is negligible.[10] These results indicate that the manganite material at the interfaces is different from that at the $LSr_{0.25}$MO core, and we conclude that only the manganite at the interfaces presents SGL behavior.

The parameters for the stretched exponentials adjusted to the data in Figs. 7(a) and 7(b) are summarized in Fig. 8, where τ and β values at 25 K are plotted as a function of t_w for both superlattices. The exponent β decreases and τ increases with t_w, indicating that a broader distribution of relaxation times is present at larger t_w. A small value of β corresponds to curves with higher initial derivative and flatter asymptotic behavior when compared to a simple exponential function. The faster relaxation indicates lower barriers against domain wall movement. The relaxation time and the exponent evolve continuously in the explored waiting time range, within the uncertainty.

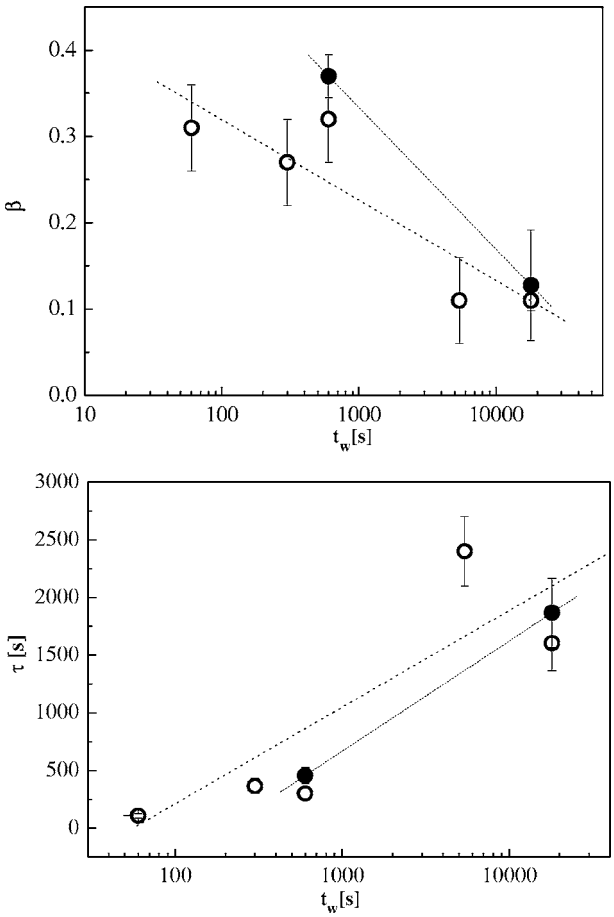

FIG. 8. Waiting time dependence of the exponent β and the characteristic time τ at 25 K. Both parameters were obtained fitting the ρ vs t curves with a stretched exponential function. Open circles: $[L_{18}P_6]_5$. Closed circles: $[L_{31}P_6]_4$. The lines in both graphics are guides to the eye.

Even though the fitted τ and β values show a high dispersion, we found they show the same trend for both superlattices, indicating that the same relaxation mechanisms are present. This could be understood considering that the frustrated manganite atomic layers responsible of the SGL behavior are close to the interface. This hypothesis is corroborated by an analysis of the magnetic viscosity. Figure 9 shows the magnetic viscosity $[S=\partial(\rho_{(t=0)}/\rho_0)/\partial\ln(t)]$ vs t dependence for the $[L_{18}P_6]_5$ and $[L_{31}P_6]_4$ superlattices and for different values of t_w. The magnitude of S is indicative of the amount of the sample that is relaxing. We observe increments of S for larger t_w, and S vs t curves that show a maximum for t values proportional to t_w. A comparison between the S value for the $[L_{18}P_6]_5$ and $[L_{31}P_6]_4$ superlattices, indicate that the relative amount of manganite that relaxes is

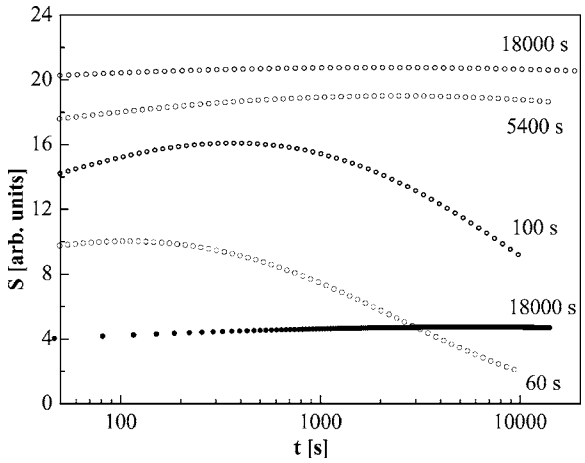

FIG. 9. Time dependence of the magnetic viscosity S for different t_w calculated from resistivity vs time measurements at 25 K. Open circles: $[L_{18}P_6]_5$. Closed circles: $[L_{31}P_6]_4$.

higher in the superlattice with thinner $LSr_{0.25}MO$ thickness.

Based in the present results our picture is that the PBCO suppresses the ferromagnetism of the $LSr_{0.25}MO$ atomic layers close to the interface, and the core $LSr_{0.25}MO$ atomic layers remain ferromagnetic. In addition the presence of the orthorhombic-rhombohedral transition enhances the intrinsic interface stress and therefore the SGL features. This structural transition is present in the superlattices, as indicated by the upturn in the resistivity curves [Fig. 6(a)]. The lack of a signature of the transition in the magnetization of the superlattices may also be due to stress at the interfaces.

SUMMARY

We present a study of the structural and magnetotransport properties for manganite or PBCO superlattices. We found that the structural disorder in these superlattices is similar to that found in ferromagnetic or superconducting superlattices. However the magnetic disorder induced at the interface is different.

The results presented show that at low temperatures the $LSr_{0.25}MO$ layers have a SGL behavior associated to a change in the stress originated by the orthorhombic-rhombohedral transition in the remaining $LSr_{0.25}MO$ ferromagnetic core.

ACKNOWLEDGMENTS

N.H., A.M.C., G.N., and J.G. acknowledge financial support from CONICET. This work was partially supported by ANPCyT Grants No. PICT2003-03-13297 and No. PICT00-03-8937, and by Fundación Balseiro, Fundación Antorchas, Argentina.

[1] P. Prieto, P. Vivas, G. Campillo, E. Baca, L. F. Castro, M. Varella, G. Ballesteros, J. E. Villegas, D. Arias, C. León, and J. Santamaria, J. Appl. Phys. **89**, 8026 (2001).
[2] Z. Sefrioui, M. Varela, V. Peña, D. Arias, C. León, J. Santamaría, J. Villegas, J. Martínez, W. Saldarriaga, and P. Prieto, Appl. Phys. Lett. **81**, 4568 (2002).
[3] H.-U. Habermeier and C. Cristiani, J. Supercond. **15**, 425 (2002).
[4] N. Haberkorn, J. Guimpel, L. B. Steren, G. Campillo, W. Saldarriaga, and M. E. Gómez, J. Appl. Phys. **94**, 3011 (2003).
[5] F. Giesen, B. Damaschke, V. Moshnyaga, K. Samwer, and G. A. Müller, Phys. Rev. B **69**, 014421 (2004).
[6] N. Haberkorn, J. Guimpel, M. Sirena, L. B. Steren, G. Campillo, W. Saldarriaga, and M. E. Gómez, Appl. Phys. Lett. **84**, 3927 (2004).
[7] P. Przyslupski, I. Komissarov, W. Paszkowicz, P. Dluzewski, R. Minikayev, and M. Sawicki, Phys. Rev. B **69**, 134428 (2004).
[8] S. Stadler, Y. U. Idzerda, Z. Chen, S. B. Ogale, and T. Venkatesan, Appl. Phys. Lett. **75**, 3384 (1999).
[9] T. Holden, H.-U. Habermeier, G. Cristiani, A. Golnik, A. Boris, A. Pimenov, J. Humlícek, O. Lebedev, G. Van Tendeloo, B. Keimer, and C. Bernhard, Phys. Rev. B **69**, 064505 (2004).
[10] N. Haberkorn and J. Guimpel, Appl. Phys. Lett. **87**, 042509 (2005).
[11] I. G. Deac, S. V. Diaz, B. G. Kim, S.-W. Cheong, and P. Schiffer, Phys. Rev. B **65**, 174426 (2002).
[12] A. Urushibara, Y. Moritomo, T. Arima, A. Asamitsu, G. Kido, and Y. Tokura, Phys. Rev. B **51**, 14103 (1995).
[13] J. Guimpel, B. Maiorov, E. Osquiguil, G. Nieva, and F. Pardo, Phys. Rev. B **56**, 3552 (1997).
[14] N. Haberkorn, F. Lovey, A. Condó, and J. Guimpel, J. Appl. Phys. **97**, 053511 (2005).
[15] P. Stadelmann, Ultramicroscopy **21**, 131 (1987).
[16] M. Hawley, I. Raistrick, J. Beery, and R. Huolton, Science **251**, 1587 (1991).
[17] R. I. Zainullina, N. G. Bebenin, A. M. Burkhanov, V. V. Ustinov, and Ya. M. Mukovskii, Phys. Rev. B **66**, 064421 (2002).
[18] P. A. Sharma, Sung Beak Kim, T. Y. Koo, S. Guha, and S-W. Cheong, Phys. Rev. B **71**, 224416 (2005).
[19] J. M. De Teresa, M. R. Ibarra, J. García, J. Blasco, C. Ritter, P. A. Algarabel, C. Marquina, and A. del Moral, Phys. Rev. Lett. **76**, 3392 (1996).
[20] R. Mathieu, P. Nordblad, D. N. H. Nam, N. X. Phuc, and N. V. Khiem, Phys. Rev. B **63**, 174405 (2001).
[21] R. S. Freitas, L. Ghivelder, F. Damay, F. Dias, and L. F. Cohen, Phys. Rev. B **64**, 144404 (2001).
[22] R. V. Chamberlin, George Mozurkewich, and R. Orbach, Phys. Rev. Lett. **52**, 867 (1984).
[23] M. Sirena, L. B. Steren, and J. Guimpel, Phys. Rev. B **64**, 104409 (2001).
[24] M. Varela, A. Lupini, S. Pennycook, Z. Sefrioui, and J. Santamaria, Solid-State Electron. **47**, 2245 (2003).
[25] P. Gaunt, J. Appl. Phys. **59**, 4129 (1986).